Medium-energy ion-scattering analysis of the $c(2\times2)$ structure induced by K on Au(110)

Patricio Häberle*
Department of Physics and Laboratory for Research on the Structure of Matter, University of Pennsylvania, Philadelphia, Pennsylvania 19104
and Department of Physics and Astronomy and Laboratory for Surface Modification, P.O. Box 849, Rutgers–The State University of New Jersey, Piscataway, New Jersey 08854

Torgny Gustafsson
Department of Physics and Astronomy and Laboratory for Surface Modification, P.O. Box 849, Rutgers–The State University of New Jersey, Piscataway, New Jersey 08854
(Received 10 May 1989)

The Au(110) surface is reconstructed and shows a (1×2) low-energy electron-diffraction (LEED) pattern, which is known to correspond to a missing-row reconstruction. At a coverage of half a monolayer of potassium, a $c(2\times2)$ LEED pattern is seen, which is not easily rationalized in terms of the faceted structures observed at lower alkali-metal coverages. Two different models have been proposed for the atomic arrangements in this structure. We have performed a medium-energy ion-scattering study, using channeling and blocking, of this surface. We find very good agreement with a model first proposed by Ho *et al.*: The top layer of atoms consists of intersecting $c(2\times2)$ arrays of Au and K atoms. The top layer of Au atoms is shifted toward the bulk, and the K atoms are displaced outward relative to this plane. The third layer of Au atoms is also buckled, all in quantitative agreement with the calculation.

I. INTRODUCTION

It is well known that the (110) surface of Au reconstructs to form a (1×2) unit cell. By a variety of techniques, most notably medium-energy ion scattering[1] (MEIS) and low-energy electron diffraction (LEED),[2] this reconstruction has been shown to correspond to a missing-row (MR) model, in which every other close-packed row of atoms along the $[\bar{1}10]$ direction is missing from the surface. This reordering is accompanied by a large inward relaxation of the remaining first-layer atoms. The (1×1) symmetry is broken also in the third layer, in that alternate rows of atoms move inward and outward in a buckling-type distortion. The net effect of the inward relaxation and the buckling is to smooth out the ragged surface profile that would otherwise arise.

Theoretical calculations of various degrees of approximation are in substantial agreement with the structural model described above.[3–7] They clearly show that the (1×1) surface is unstable toward reconstruction and that higher-order reconstructions [(1×3), (1×4), etc.] have energies very close to (1×2).[4,5,7] We were recently able to induce two such superstructures, namely, a (1×5) and a (1×3) structure, by adsorbing very small amounts [≈0.03 and 0.05 monolayers (ML), respectively] of cesium.[8] In a detailed study, we were able to show that the structure of the (1×3) surface corresponds to a "generalized missing-row model," in which two adjacent rows of atoms are missing in the first layer and another row of atoms is missing in the second layer. The resulting surface will therefore have large (111)-like facets, which presumably are quite stable. Also, here, we find clear evidence for an inward relaxation of the first layer of atoms and a buckling in the third layer.[8] This structure is in agreement with theoretical expectations.[4,5,9] It is also quite similar to a recently proposed model for a (1×3)-induced reconstruction of Pt(110), although the agent that causes the reconstruction in that case has not been identified.[10] The (110) surfaces of the 3*d* fcc metals, for example Cu and Ni, are unreconstructed [(1×1) LEED patterns], as are the 4*d* fcc (110) surfaces, like Pd and Ag. However, many of these surfaces can also be induced to reconstruct to a (1×2) MR structure by adsorption of submonolayer amounts of alkali metals.[11–14] It has been suggested that the role of the alkali metal is mainly that of a charge donor, which shifts the delicate balance between *d* bonding and *sp* bonding at the surface. Therefore, one expects the alkali-metal atoms to be predominantly ionic.

At large alkali-metal coverages, the repulsion between alkali-metal ions will become important, and the alkali-metal-substrate bond should rather be metallic in character. In a recent report, a striking similarity was observed in a sequence of LEED patterns for increasing amounts of K adsorbed on Ni(110) and on Au(110).[15] An ordered $c(2\times2)$-overlayer pattern shown by both systems is especially interesting. For K/Ni(110), the LEED pattern was assigned to an overlayer formed by 0.5 ML of K atoms adsorbed in the troughs on a (1×1) Ni(110) substrate, the symmetry of which does not change during the adsorption. Since K/Au(110) showed the same sequence of LEED patterns, the same model was also proposed for the $c(2\times2)$ pattern on Au(110). In this case, the adlayer must have induced substantial reordering in the sub-

strate. The absence of half-order (01)-type spots implies that a structural change of the Au substrate must occur, since a (1×2) surface is incompatible with a $c(2\times2)$ pattern. We will refer to this model as the *overlayer model* [Fig. 1(a)]. This interpretation was later supported by a calculation using the effective-medium theory (EMT).[9] One result of this calculation was that alkali-metal overlayers, which at low coverages favor a MR structure, stabilize the bulk termination of the fcc(110) surfaces at high coverages. A different model was later proposed by a first-principles calculation.[16] In this model the top layer consists of an ordered surface alloy of alternating K and Au atoms forming close-packed rows along the $[\bar{1}10]$ direction. Since the $c(2\times2)$ structure evolves from a MR model, the new structure can then be thought of as being formed by breaking up the close-packed Au rows, displacing every other Au atom to the nearest vacant position on the "missing rows" and putting K atoms on the remaining top-layer sites. We will refer to this model as the *substitutional model* [Fig. 1(b)].

Symmetry-based arguments like those presented in favor of the overlayer model are quite attractive, but experience has shown that it is always useful to perform a direct structural study, where the positions of the surface atoms are measured directly. Below we therefore present our results from an experimental study with medium-energy ion scattering with channeling and blocking of the $c(2\times2)$ K-induced reconstruction of Au(110). The strength of MEIS is that it is a quantitative structural technique, in that the ion-solid–interaction law is accurately known in the energy range used, and that often useful structural information can be obtained by merely inspecting the data.[17] We have analyzed our data, both in qualitative terms and with the aid of detailed Monte Carlo simulations of different trial structures, in an attempt to differentiate between the two models. In Sec. II we describe the experimental setup and sample preparation. The results, which clearly favor the substitutional model, are presented in Sec. III. In Sec. IV we give a brief summary.

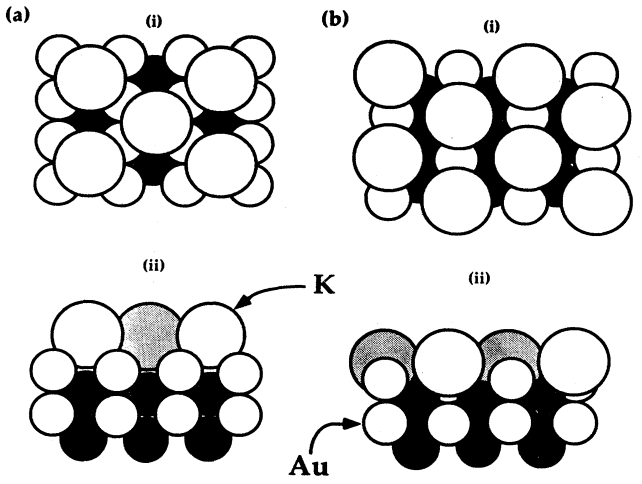

FIG. 1. (a) Top, (i), and side view, (ii) [in the $(\bar{1}10)$ plane], of the $c(2\times2)$ structure in the overlayer model. (b) Same as in (a), but for the substitutional model.

II. EXPERIMENT

A schematic picture of the surface of a (1×1) fcc (110) surface is given in Fig. 1. The ion beam is incident on the target in a low-index crystallographic direction. The intensity and angular dependence of the backscattered ion flux is determined as a function of backscattered ion energy for a fixed incidence energy. The experimental setup[18] consists of an ultrahigh-vacuum (UHV) chamber, equipped with facilities for LEED; Auger spectroscopy, a K source, a quadrupole mass spectrometer (QMS), etc. The sample is mounted on a high-precision three-axis goniometer, which allows the alignment of the crystal with the desired scattering plane with an accuracy of 0.01°. The ion energies are measured with a rotatable, commercial, toroidal energy analyzer, which is attached to a 180-keV ion accelerator via a differentially pumped beam line. Ion energies as low as 50 keV were used, and the only ion species utilized was protons.

The Au crystal was mechanically polished and then electropolished in a cyanide solution. An x-ray analysis showed that a (110) axis was within 1° of the surface normal. The sample was cleaned with standard procedures.[1,8] The K source (SAES Getters USA) was heated resistively at a constant current to produce a deposition rate of approximately 0.2 ML/min. We performed a preliminary sample-preparation study in a separate UHV system. There, the alkali-metal-induced work-function change was measured from the low-energy cutoff of the electron current from a variable-energy, low-energy electron gun. Usually, several monolayers were deposited with the sample at room temperature. A thermal-desorption-spectroscopy (TDS) spectrum for such a sample would show a multilayer K desorption peak around 485 K. It was found that a sample that showed a clear peak in the TDS spectrum subsequently showed a good-quality $c(2\times2)$ LEED pattern. In experiments in the main experimental chamber the coverage was monitored using ratios of the K and Au Auger intensities, which were put on an absolute scale using the ion-backscattering signal as explained below.

The raw data were normalized by comparing them with a calibrated standard. They were also corrected for the (energy-dependent) ion-neutralization probability using a solid-state detector and a set of electrostatic deflection plates. After division with the smooth Rutherford cross section, the yield can be compared to Monte Carlo simulations of the experiment for various trial structures without the introduction of arbitrary scaling constants. By comparing simulations and data using an R-factor analysis,[8,19] the structural parameters of the surface can be determined.

The major uncertainty in the modeling of the ion-solid interaction arises from the difficulty in modeling the enhancement of the thermal vibration amplitudes at the surface. Following earlier work,[8,17,19] we have assumed, both for the bulk and the surface, that these amplitudes

are isotropic and follow a Gaussian distribution, characterized by a one-dimensional standard deviation, u_{one}, around the equilibrium positions. The bulk one-dimensional vibrational amplitude of Au is, at 300 K, 0.087 Å. To account for correlations in vibrational motions between adjacent atoms, we have rescaled the bulk vibrations:[20] u_{one} (with correlations) $=u_{one}$(uncorrelated)$\sqrt{1-c_{NN}}$ with a nearest-neighbor correlation factor (c_{NN}) of 0.30, also taken from bulk data.[21]

In principle, we should consider the vibrational amplitude of every atom in the unit cell as an independent variational parameter in the simulations on the same standing as the structural parameters. This approach is impractical because it will increase the computational time very substantially. In previous simulations we have found the influence of the vibrational parameters to be secondary to that of the structural parameters. We therefore used only two parameters to describe the vibrations, namely the vibrational amplitude of the K atoms and an enhancement amplitude. The latter assigns a common value to the amplitude in the first three layers of the substrate (u_s). The amplitude of the thermal vibrations in fourth and deeper layers was assigned the bulk value.

III. RESULTS

The alkali-metal coverage is determined by measuring the number of ions backscattered from the adsorbate into a particular detection angle for a given beam dose and comparing it to a similar measurement done on a calibration standard. The ions backscattered from the K atoms at the surface appear in the spectrum at a lower energy than the Au surface peak. This is a purely kinematic effect due to the lower mass of K relative to that of Au. The K surface peak will therefore sit on top of a background intensity coming from ions backscattered by Au atoms in deeper layers of the crystal. To minimize the effect of the background and get a better estimate of the coverage, we measured the K peak at a scattering angle ($70.5°\pm0.1°$) that corresponds to a bulk blocking direction (double alignment) in the ($\bar{1}10$) scattering plane (see Fig. 2). The results are shown in Fig. 3, where the shaded area at 62.3 keV corresponds to the signal from the K adsorbate. After proper normalization of the yield and averaging over 10 angular channels ($\approx 2°$), we found the area under the K peak to be equivalent to 0.53 ± 0.03 ML (1 ML$=8.5\times10^{14}$ atoms/cm^2). Both the substitutional model and the overlayer model imply a coverage of 0.5 ML [one K atom every two (1×1) surface unit cells]. To differentiate between these models, we should therefore look at the yield as a function of scattering angle.

In order to understand the data below, it is useful to remember that the Rutherford scattering cross section is proportional to the square of the nuclear charge Z. A K atom ($Z=19$) will therefore have a cross section a factor of 17 smaller than a Au atom ($Z=79$). This implies that to a first approximation, the ion beam will only see the Au atoms and not the K adsorbates. Slightly simplified, for the purposes of ion scattering, the overlayer model will therefore correspond to a (1×1) Au surface, while the substitutional model will correspond to a $c(2\times2)$ array of Au atoms on a Au substrate.

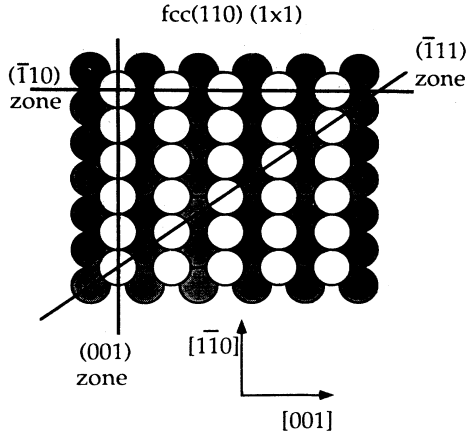

FIG. 2. Top view of a fcc (110) bulk-terminated surface [(1×1) surface structure]. The solid lines indicate the different scattering planes used in this study.

The scattering plane or zone which provides the most information is the ($\bar{1}10$) zone. The data (Fig. 4) show clear blocking dips along the [112] and [114] directions. The scattering yield stays well below 2.0 atoms/(unit cell) in the [114] direction and shows no structure (blocking dips or peaks) for scattering angles smaller than 48.5°, which corresponds to the [116] blocking direction. This low-angle behavior is completely different from what has been observed for the (1×2) surface, where the [118] blocking dip shows up very clearly in the data.[1] There is

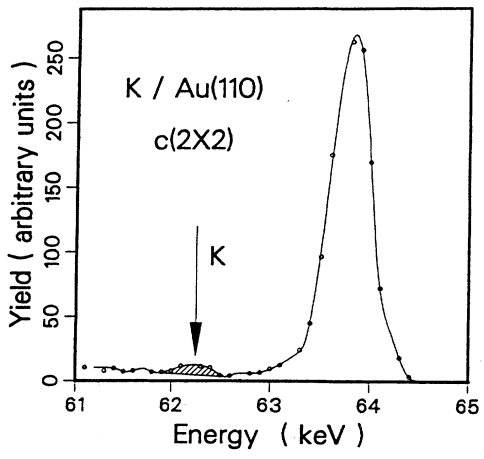

FIG. 3. Energy distribution of the backscattered flux of 64.3-keV protons from the $c(2\times2)$ K-induced reconstruction of Au(110). The protons were incident along the [$\bar{1}\bar{1}2$] direction and detected along the [112] direction (equivalent to a scattering angle of 70.5°). The dashed area corresponds to the protons backscattered from the K atoms on the surface, while the peak at 63.8 keV is the Au surface peak.

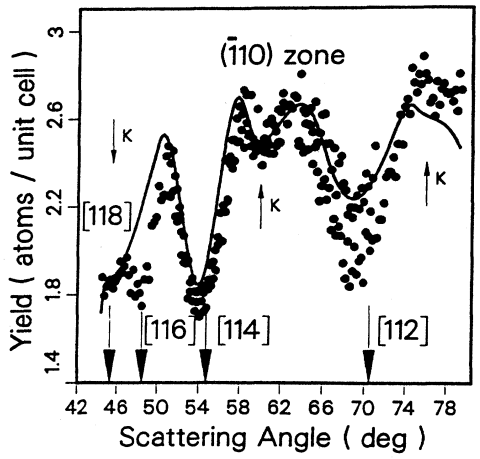

FIG. 4. Experimental yield for 65-keV protons incident in the ($\bar{1}10$) zone along the [$\bar{1}\bar{1}2$] direction as a function of scattering angle. The data for the $c(2\times2)$ surface are shown with solid circles. Note that the blocking-dip minima are shifted with respect to the bulk [112] and [114] crystallographic directions. A simulation of the scattering yield for our best structure (solid line) is also shown.

also a weak blocking dip around 60°, an angle which does not correspond to a Au bulk blocking direction.

Figure 1(a) shows the structure of the overlayer model in the ($\bar{1}10$) zone. The positions of the K atoms are assumed to be far from the Au lattice sites (this holds regardless of the structural model) because the K atoms have much larger radii than the Au atoms. For a (1×1) Au surface, and neglecting thermal vibrations for the moment, the ion beam will see 2 atoms/(unit cell). As these two atoms are in different scattering planes in this zone, blocking will not reduce the scattering yield below this value at any angle. Nonzero thermal vibrations and/or distortions of atomic positions away from the bulk positions can only increase the hitting probability beyond 2 atoms/(unit cell). Experiments on the (1×1) structures of Ag(110) (Ref. 22) and Cu(110) (Ref. 23) indeed show that the smallest value of the backscattered yield in this zone is between 2.1 and 2.2 atoms/(unit cell). Our Monte Carlo calculations for a Au(110) surface with a (1×1) termination show a slightly larger value for the smallest yield in this zone [between 2.2 and 2.3 atoms/(unit cell)]. This is due to the fact that Au has a lower Debye temperature than Cu or Ag. Experimentally, the yield from this zone has, instead, a minimum value of 1.8 atoms/(unit cell), well below the lower limit for a (1×1) structure. Even if we were to assume that the K atoms on the surface are located at positions where they can contribute significantly to the blocking, say in the [114] direction, 0.5 ML of K atoms cannot block effectively enough to cause the observed low yield. *This observation eliminates the overlayer as a possible model for the structure of this surface.*

The low values of the yield indicate instead that there should be vacancies in the top layer, which allow the incident ions to get below the first layer of the crystal. These ions are scattered from deeper layers and then blocked on their way out of the crystal by the remaining Au atoms in the top layer, reducing the yield in the blocking directions. The substitutional model contains features to explain this. In the substitutional model [Fig. 1(b)], the incident ions will penetrate unimpeded through the vacancies beyond the first layer of the crystal. The backscattered flux from the third-layer atoms is then blocked along the [114] direction, causing a deep blocking dip. The blocking in the [112] direction is not as strong as in the [114] direction because the flux being blocked comes from atoms that are only partially "seen" by the incoming beam. The qualitative features of the substitutional model therefore agree well with the measured data.

Figure 5 shows data obtained from the (001) scattering plane with the ion beam incident along the [0$\bar{1}$0] direction. Figure 6 shows the arrangement of the surface atoms in the substitutional model in this zone. Topologically, the arrangement of the atoms is then very similar in the (001) and ($\bar{1}10$) zones [Figs. 1(b) and 6]. The [112], [114], and [116] directions in the (110) zone are equivalent to the [100], [3$\bar{1}$0], and [2$\bar{1}$0] directions, respectively, in the (001) zone. The interatomic distances are different, though. The main differences in the scattering yield between the two zones are observed for lower scattering angles. Here the ($\bar{1}10$) zone shows a slightly lower yield. This difference comes from the (weak) blocking by the K adlayer of the flux backscattered from the first-layer Au atoms. For the K-Au distance ($d_{\text{K-Au}}$) found from the simulations (as explained below), this effect becomes significant for scattering angles smaller than 51° in the ($\bar{1}10$) zone, compared to 66° in the (001) zone. Another manifestation of K blocking is the weak, but distinct, blocking dip around 80°. This angle corresponds to no bulk blocking direction in Au. Our simula-

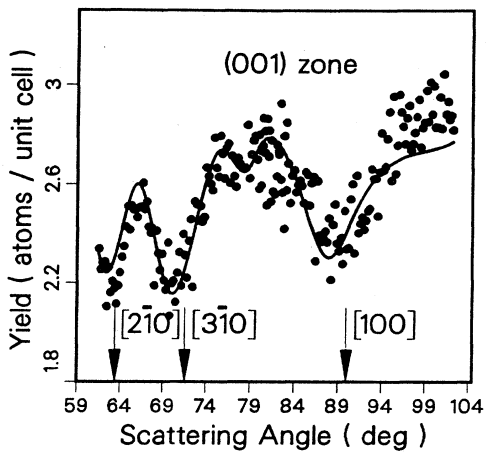

FIG. 5. The experimental yield for 65-keV protons incident in the (001) zone along the [0$\bar{1}$0] direction as a function of scattering angle. The bulk blocking directions ([100], [3$\bar{1}$0], and [2$\bar{1}$0]) are indicated. The solid line is the simulation for the best structure.

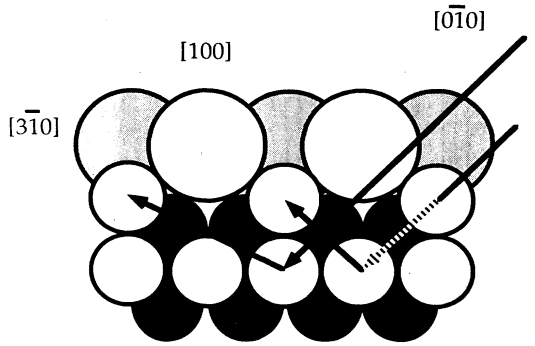

FIG. 6. Side view [in the (001) plane] of the substitutional model. The top layer is formed by alternate Au and K atoms. The arrows show ions trajectories for the main blocking directions ([100] and [3$\bar{1}$0]). The interrupted line indicates a trajectory partially blocked in the [0$\bar{1}$0] channeling direction by a top-layer Au atoms.

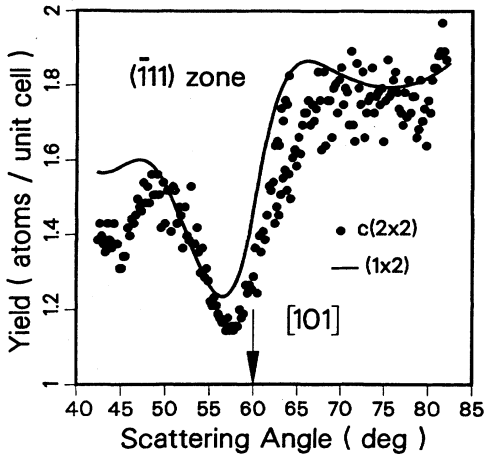

FIG. 7. Experimental yield for 65-keV protons incident in the ($\bar{1}$11) zone along the [0$\bar{1}$1] direction as a function of scattering angle. The bulk [101] blocking direction is indicated. The solid circles are the data for the $c(2\times2)$ surface structure. The line is a spline fit to the data for the clean (1×2) surface. Notice the shift of the blocking dip to lower scattering angles in both cases.

tions show that it is associated with Au blocking by the K atoms.

The [110] blocking dip in the (001) zone and the [112] blocking dip in the ($\bar{1}$10) zone are both shifted slightly to smaller scattering angles. As the location of blocking dips in this geometry is a measure of the distance between the first and third layer (d_{13}), this implies a contraction of d_{13}. This is in contrast to what was observed on the (1×2) surface,[1] but similar to what we saw on the (1×3).[8] This effect is not as pronounced in the [114] and [3$\bar{1}$0] blocking dips because of averaging due to additional surface distortions. We will find below that there is a very important buckling distortion of the third layer (B_3), which opposes the effects of the contraction of d_{13} in the data around the [114] and [310] directions.

Data from the ($\bar{1}$11) zone (Fig. 2) are presented in Figs. 7 and 8. The ions were incident along the [0$\bar{1}$1] direction and the detector was centered around the [101] direction. The [101] bulk blocking direction is located at 60°. The solid line in Fig. 7 is a spline fit to data for the same zone for the (1×2) surface. A feature of the substitutional model is that there are two distinct atomic planes contributing to the scattering (see Figs. 2 and 9). One of these planes has exclusively potassium atoms in the top layer, while the other plane corresponds to a gold-terminated structure. The most significant aspect of the data is a shift of the blocking dip to scattering angles lower than the bulk value. This is clear evidence of a contraction of an interlayer distance. For the substitutional model the observed shift comes from the contributions of two interlayer distances in that changes of d_{12} and d_{23} both contribute to the position of the blocking-dip minimum in this zone. For the overlayer model the observed shift comes mainly from d_{12}. The angular shift of the blocking dip is larger for the (1×2) surface[1] than for the $c(2\times2)$ phase, indicating a smaller contraction in the $c(2\times2)$ case than for the clean surface.

We did extensive Monte Carlo simulations and an R-factor analysis for the scattering yield in the ($\bar{1}$11), ($\bar{1}$10), and (001) zones.[24] For the Au substrate, we varied the following parameters: d_{12}, d_{23}, d_{34}, B_3, and u_s [Fig. 9(b)]. For the K atoms, we varied the vibrational amplitude and the vertical position of the K relative to the Au surface. Our results show a contraction of d_{12}, $\Delta d_{12}=(-13\pm3)\%$. The second-largest distortion is a buckling in the third layer, $B_3=(8\pm3)\%$. The buckling is such that the third-layer atoms below the top-layer Au atoms move from the average third-layer position toward the bulk by 4% of the bulk interlayer distance, and the third-layer atoms underneath the K atoms move toward the surface by the same amount. We also found a (possible) contraction of the second-interlayer distance d_{23},

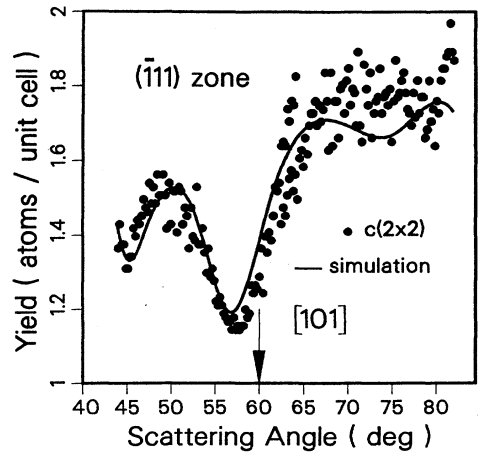

FIG. 8. Data (solid circles) and simulation (solid line) of the backscattered yield for the $c(2\times2)$ structure in the ($\bar{1}$11) zone. The [101] bulk blocking direction is indicated.

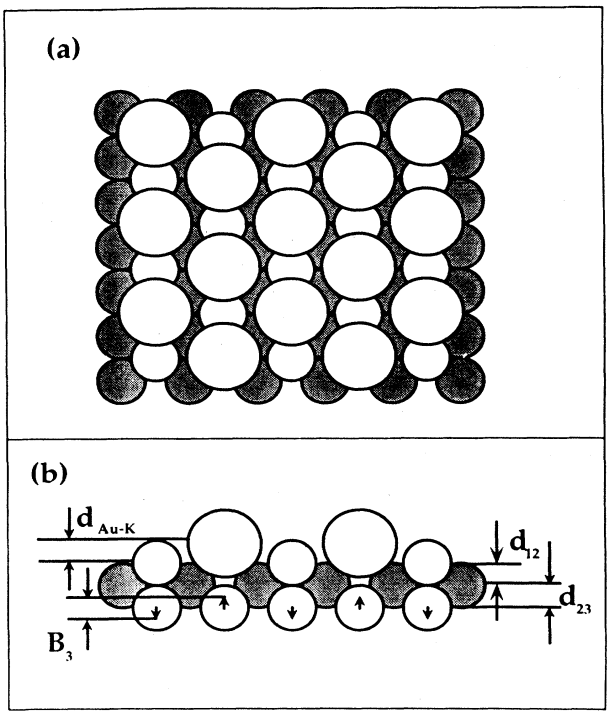

FIG. 9. (a) Top view of the substitutional model. The larger circles represent the K atoms. (b) Side view in the $(\bar{1}10)$ zone. The vertical arrows in the third Au layer indicate the relative directions of movement of the atoms.

$\Delta d_{23}=(-4\pm5)\%$, and a distance between the third and fourth layers consistent with the bulk interlayer distance, $\Delta d_{34}=(0\pm4)$. Our data were best fitted with an effective thermal vibrational amplitude for the Au surface (u_s) of 0.17 ± 0.02 Å.

The K atoms have been included in all the Monte Carlo simulations actually performed to search for the best structural parameters. To understand the extent to which the presence of K atoms can be neglected, we did additional simulations without K atoms in the top layer. As an example, we will consider the results for the $(\bar{1}10)$ zone. In Fig. 4 we have indicated with arrows the regions where the largest differences induced by the K atoms occur. One effect of the K atoms is to increase the yield by 0.10–0.15 atoms/(unit cell) in this region. This is anticipated since some of the outgoing ions are blocked by the K atoms. The depths of the K-induced dips are, as expected, small, but give us sensitivity to the position of the K adlayer above the Au substrate. The vertical distance between the K atoms and the first Au layer [Fig. 9(b)] was found, from the Monte Carlo simulations, to be $d_{K\text{-}Au}=1.05\pm0.15$ Å. Based on this measurement we can calculate a radius of the K atom: $r_K=2.0\pm0.2$ Å. This value should be compared to the K atomic radius ($r_K^{at}=2.26$ Å), the ionic radius ($r_K^{ion}=1.33$ Å), and the radius shown by K in the only known stable alloy between Au and K, Au_5K (1.85 Å). The one-dimensional vibrational amplitude associated with the K atoms obtained from the simulations is 0.21 ± 0.03 Å. The large error bars in the parameters associated with the adatoms are a consequence of the low sensitivity of the backscattered yield to the K atoms. Our results are summarized in Table I.

The errors for the structural parameters quoted above reflect two sources only:[8] (1) the range over which the structural parameters can be changed without visually affecting the quality of the fit to the data in a given zone, and (2) the differences in the optimum structural parameters in different scattering zones. The large error bar on Δd_{23} is mostly due to the latter effect as we obtain a significantly larger contraction of d_{23} in the $(\bar{1}11)$ zone than in the $(\bar{1}10)$ and (001) zones. For the substitutional model, the $(\bar{1}11)$ zone is very sensitive to defects. This sensitivity comes from atomic planes with a top layer formed exclusively by K atoms. If we replace some of the K atoms with Au atoms (<0.10 ML), we obtain better agreement between data and simulation. This can be understood by examining the simulation for the perfect structure. The solid line in Fig. 8 is the simulation for the substitutional model in the $(\bar{1}11)$ zone. The simulation single-alignment yield for scattering angles between 68° and 83° is slightly lower than the data. If we substitute Au atoms for K atoms, this will increase the single-alignment yield because the number of Au atoms in this plane will be larger than for the perfect substitutional structure. At the same time the [101] blocking dip will get deeper.

Chan and Ho[16] obtained from their self-consistent calculation that the substitutional model had a considerably lower energy than the overlayer model. Furthermore, they found a contraction on the first-layer spacing $\Delta d_{12}=-15.9\%$, and predicted the buckling in the third layer (B_3) to be 7%. The position of the K atoms was found to be 1.08 Å above the top Au layer. The agreement between the calculation and our measured parameters is therefore extremely good. The calculation also gave an expansion of the second-layer spacing, $\Delta d_{23}=+5.3\%$, while our data tend to indicate that d_{23} is contracted, although the error bar is quite large. The difference is possibly related to the fact that their calculation only involved a finite number of layers.

The relaxations measured for the $c(2\times2)$ structure are smaller than those measured for the clean Au(110) (1×2) surface.[1] This agrees with the trend shown by the relaxations in the fcc (110) surfaces, where larger relaxa-

TABLE I. Surface distortions of Au(110).

	K/$c(2\times2)$ Calc.[a]	K/$c(2\times2)$ MEIS[b]	(1×2) MEIS[c]
Δd_{12} (%)	−15.9	-13 ± 3	−18
B_3 (%)	+7	$+8\pm3$	+14
Δd_{23} (%)	+5.3	-4 ± 5	+4
$d_{K\text{-}Au}$ (Å)	1.08	1.05 ± 0.15	

[a]Reference 16.
[b]Results of the present study.
[c]Reference 1.

tions occur on more open, reconstructed surfaces. The main distortions found on the (1×2) surface were a contraction of the first-interlayer distance, $\Delta d_{12}=-18\%$, and a buckling of the third layer, $B_3=14\%$.[1] There is some model dependence in the values that can be obtained from a Monte Carlo simulation of MEIS data, but at the same time there are constraints. The position of a blocking-dip minimum cannot be reproduced unless the atoms at the surface have a very definite relative position. This will imply, for example, that the value we measure for $\Delta d_{12}(-13\%)$ cannot vary over a wide range if we change the structural model. The relaxations of the bulk-terminated (1×1) fcc (110) surfaces, on the other hand, have values in the range $\Delta d_{12}=-5.0$ to -9.0%. We would expect, then, for a clean Au(110) (1×1) bulk-terminated structure a similar relaxation. In addition, adlayers tend to decrease the contraction of d_{12}. Therefore, for a (1×1) Au(110) surface with 0.5 ML K adsorbed on top, we certainly expect a value at the lower end of this range. The fact that the $c(2\times2)$ structure presents a larger relaxation than those shown by the bulk-terminated structures is then another argument in favor of the substitutional model.

IV. SUMMARY

We found the absolute value of the K coverage corresponding to the $c(2\times2)$ pattern to be $\Theta_{\text{sat}}=0.53\pm0.03$ ML. From the MEIS data for this structure, we observed direct and clear evidence for vacancies in the top layer of Au atoms, in agreement with the substitutional model proposed by Ho *et al.*[16] to explain this surface reconstruction. Direct evidence for a substantial contraction of the first layer can also be obtained by inspection of the experimental data. As a result of the Monte Carlo simulations, we find that the two main distortions are a contraction of the first-Au-interlayer distance, $\Delta d_{12}=(-13\pm3)\%$ and a buckling of the third layer, $B_3=(8\pm3)\%$. The top layer of atoms is rippled, with the K nuclei located 1.05 ± 0.15 Å above the Au nuclei. The values of these distortions are in exceptionally good agreement with the predictions of Ho *et al.*[16] The radius of the K atom (2.0 ± 0.2 Å) is slightly smaller than that of bulk potassium, but very significantly larger than the ionic radius.

ACKNOWLEDGMENTS

We thank Dr. K. M. Ho and Dr. C. T. Chan for communicating their results in advance of publication and for permitting us to quote them here. We would also like to thank Dr. P. O. Nilsson for supplying the crystal used in this work and Mr. P. Fenter for helpful discussions. This research was supported by the U. S. National Science Foundation under Grant No. DMR-87-03897. Use of the Central Facilities at the Laboratory for Research on the Structure of Matter at the University of Pennsylvania, under Grant No. DMR-85-19050, is gratefully acknowledged.

*Present address: Departamento de Física, Universidad Técnica Federico Santa María, Casilla 110-V, Valparaíso, Chile.

[1] M. Copel and T. Gustafsson, Phys. Rev. Lett. **57**, 723 (1986).
[2] W. Moritz and D. Wolf, Surf. Sci. **163**, L655 (1985).
[3] J. W. Davenport and M. Weinert, Phys. Rev. Lett. **58**, 1382 (1987).
[4] F. Ercolessi, A. Bartolini, M. Garofalo, M. Parinello, and E. Tosatti, Phys. Scr. T **19B**, 399 (1987).
[5] M. Garofalo, E. Tosatti, and F. Ercolessi, Surf. Sci. **188**, 321 (1987).
[6] K.-M. Ho and K. P. Bohnen, Phys. Rev. Lett. **59**, 1833 (1987).
[7] S. M. Foiles, Surf. Sci. **191**, L779 (1987).
[8] P. Häberle, P. Fenter, and T. Gustafsson, Phys. Rev. B **39**, 5810 (1989).
[9] K. W. Jacobsen and J. K. Nørskov, Phys. Rev. Lett. **60**, 2496 (1988).
[10] P. Fery, W. Moritz, and D. Wolf, Phys. Rev. B **38**, 7275 (1988).
[11] M. Copel, W. R. Graham, T. Gustafsson, and S. Yalisove, Solid State Commun. **54**, 695 (1985).
[12] B. E. Hayden, K. C. Prince, P. J. Davie, G. Paolucci, and A. M. Bradshaw, Solid State Commun. **4**, 325 (1983).
[13] C. J. Barnes, M. Q. Ding, M. Lindroos, R. D. Diehl, and D. A. King, Surf. Sci. **162**, 59 (1985).
[14] J. W. M. Frenken, R. L. Krans, J. F. van der Veen, E. Holub-Krappe, and K. Horn, Phys. Rev. Lett. **59**, 2307 (1987).
[15] R. J. Behm, D. K. Flynn, K. D. Jamison, G. Ertl, and P. A. Thiel, Phys. Rev. B **36**, 9267 (1987).
[16] K. M. Ho and C. T. Chan, Bull. Am. Phys. Soc. **33**, 396 (1988); K. M. Ho, C. T. Chan, and K. P. Bohnen (unpublished).
[17] J. F. van der Veen, Surf. Sci. Rep. **5**, 199 (1985).
[18] W. R. Graham, S. M. Yalisove, E. D. Adams, T. Gustafsson, M. Copel, and E. Törnqvist, Nucl. Instrum. Methods B **16**, 383 (1986).
[19] P. Fenter and T. Gustafsson, Phys. Rev. B **38**, 10 197 (1988).
[20] D. P. Jackson, T. E. Jackman, J. A. Davies, W. A. Unertl, and P. D. Norton, Surf. Sci. **126**, 226 (1983).
[21] S. P. Withrow, J. H. Barrett, and R. J. Culbertson, Surf. Sci. **161**, 584 (1985).
[22] E. Holub-Krappe, K. Horn, J. W. M. Frenken, R. L. Krans, and J. F. van der Veen, Surf. Sci. **188**, 335 (1987).
[23] M. Copel, T. Gustafsson, W. R. Graham, and S. M. Yalisove, Phys. Rev. B **33**, 8110 (1986).
[24] P. Häberle, Ph.D. thesis, University of Pennsylvania, 1989 (unpublished).